INTERNATIONAL JOURNAL OF INNOVATIVE COMPUTING
ISSN 2180-4370
Journal Homepage : https://ijic.utm.my/

New Proposed Mixed Transforms: CAW and FAW and Their Application in Medical Image Classification

Maryam I Mousa Al-Khuzaay
Informatics Institute for Postgraduate Studies
Iraqi Commission for Computer and Informatics
Baghdad, Iraq
Email: Phd2020300561@iips.icci.edu.iq

Waleed A. Mahmoud Al-Jawher
Uruk University
Baghdad, Iraq

Submitted: 30/11/2022. Revised edition: 31/3/2023. Accepted: 31/3/2023. Published online: 13/9/2023
DOI: https://doi.org/10.11113/ijic.v13n1-2.414

***Abstract*—The transformation model plays a vital role in medical image processing. This paper proposed new two Mixed Transforms models that are the hybrid combination of linear and nonlinear Transformations techniques. The first mixed transform is computed in three steps: calculate 2D discrete cosine transform (DCT) of the image, and applying Arnold Transform (AT) on the DCT coefficients, and applying the discrete Wavelet Transform (DWT) on the result to get which was abbreviated as (CAW). The second mixed transform consists of firstly computing the discrete Fourier transform (DFT), net applying the Arnold Transform (AT), and finally, the computation of discrete Wavelet Transform (DWT) which was abbreviated as (FAW). These transforms have superior directional representations as compared to other multiresolution representations such as DWT or DCT and work as non-adaptive mixed transformations for multi-scale object analysis. Due to their relationship to the wavelet idea, they are finding increasing use in areas like image processing and scientific computing. These transforms are tested in medical image classification task and their performances are compared with that of the traditional transforms. CAW and FAW transforms are used in the feature extraction stage of a classification VGG16 deep learning (DNN) task of Tumor MRI medical image. The numerical findings favor CAW and FAW over the wavelet transform for estimating and classifying pictures. From the results obtained it was shown that the CAW and FAW transform gave e much higher classification rate than that achieved with the traditional transforms, namely DCT, DFT and DWT. Furthermore, this combination leads to a family of directional and multi-transformation bases for image processing.**

***Keywords*—CAW, FAW, VGG16, DNN, DWT**

I. INTRODUCTION

Cosine and Fourier transforms are useful in obtaining excellent information from periodic signals than other transforms. Wavelet transform families are effective in dealing with multi-spectrum data than Cosine and Fourier transforms. Ridgeley transform show much better representation than Cosine, Fourier and Wavelet transforms but with very high computation complexity. Hence a proper merging technique of these transforms approach with their cascaded application will extract useful information from the signals under consideration.

The Artificial Neural Network is trained with cutting parameters, vision parameters as input and the experimental surface roughness (Ra, Rq, Rz) as output. The validation results of proposed models show better performance with reasonable accuracy.

It is obvious in signal processing field that it is possible to gain insight into the most dominating frequency components of any wavelet coefficients decomposition levels through the application of DCT and DFT. This feature is highly essential in signal processing applications for the in-depth analysis on input signal components. Hence, the cascaded application of theses transforms will have the hybrid features that result in obtaining the frequency spectrum of any level of wavelet coefficients. The novel feature of this technique becomes more evident for any signal processing application.

A. Discrete Wavelet Transform (DWT)

The DWT method is an image/frame transform technique that uses multiresolution and orthogonal transformations. This transformation method is excellent for transforming signals in the spatial domain to coefficients in the frequency domain. Input images and frames may be broken down into horizontal, vertical, and diagonal bands using the wavelet transform. These bands are labelled LL, LH, HL, and HH. In a picture or frame, the low frequency band (LL) represents an approximation, while the high frequency bands (LH, HL, and HH) depict the finer details [16], [17], [18].

B. Discrete Cosine Transform

In order to construct a finite series of cosine function forms at different frequencies, a Discrete Cosine Transform (DCT) might be quite helpful. It's a way of breaking down any signal into its fundamental frequency components. DCT is a block-based transformation method that splits the image/frame into NN non-overlapping chunks. The DCT coefficients for an input picture X and an output image Y (of size N M) may be determined using Eq. (1):

$$Y(u,v) = \sqrt{\frac{2}{m}}\sqrt{\frac{2}{n}}\alpha\sum_{m=0}^{M-1}\sum_{n=0}^{N-1}X(m,n)cos\frac{(2m+1)u\pi}{2m}cos\frac{(2n+1)v\pi}{2n} \quad (1)$$

Where

$$\alpha = \frac{1}{\sqrt{2}} for, u\&v = 0$$

$$\alpha = 1\, for, u\&v = 1,2, \dots, M-1$$

In terms of continuity, DCT outperforms DFT. Comparatively, DFT is a periodic representation of the signal with truncation of coefficients[19], whereas DCT is beneficial for representing the signal with a minimal number of coefficients[20].

C. Arnold Transform

FAN Transform is a scrambling protection method for image encryption. A special of FAN that based on Arnold Transform, possesses wide range of transform matrix which is called FAN transform-set. The expression of FAN Transform-set is given below:

$$\begin{pmatrix} y_1 \\ y_2 \end{pmatrix} = \begin{bmatrix} a_{00} & a_{01} \\ a_{10} & a_{11} \end{bmatrix}\begin{pmatrix} x_1 \\ x_2 \end{pmatrix} + k\begin{pmatrix} N \\ N \end{pmatrix} \bmod N \quad (2)$$

As a special case that satisfy formula (2) in FAN Transform, one can achieve Arnold Transform, where,

$$\begin{pmatrix} y_1 \\ y_2 \end{pmatrix} = \begin{bmatrix} 1 & 1 \\ 1 & 2 \end{bmatrix}\begin{pmatrix} x_1 \\ x_2 \end{pmatrix} + k\begin{pmatrix} N \\ N \end{pmatrix} \bmod N \quad (3)$$

The values of the original signal are randomised by applying the periodic Arnold transform. As a result, it might be used for a variety of different purposes within the context of information concealment methods.

The original image's pixel value is denoted by (y 1, y 2), whereas the [21] image's pixel value is denoted by (x 1, x 2). picture is N by N, or a square image; if it is not, you may always adjust it to fit into a square. It makes an effort to reorganize the original image's pixels. Because the picture is represented as a matrix of discrete points, it may be rebuilt by repeatedly applying the Arnold transforms to the same steps or applying the inverse transformation to the same steps. This demonstrates the cyclical character of the change. When the size of the picture is expanded by a factor of N, the radius of the circle used in the transformation will also grow by N. When it comes to boosting security, Arnold transform is simpler to apply and has shown to be useful [22].

D. Fast Fourier Transform

The discrete Fourier transform (DFT) is a tool for converting certain kinds of sequences of functions into other kinds of representations, and a fast Fourier transform (FFT) is an algorithm that calculates the DFT of some sequence. Discrete Fourier transform may also be seen as the process by which a wave's cyclical structure is converted into its constituent sine waves. Comparatively speaking, calculating the DFT using FFT is much quicker than simply processing the input. When applied to a problem of size N, the FFT decreases the amount of calculations required from O(N2) to O(NlogN) [23].

E. VGG16

CNN has become more and more effective in the field of image classification. In 2014, Simonyan and Zisserman proposed an easy and efficient CNN design principle called VGG[24].VGG architecture is based on increasing depth using a number of successive layers. It is one of the most popular pre-trained models for image classification that was presented at the famous ILSVRC 2014 conference, and it was and still is the model that should produce more accurate results today. Developed at Oxford University's Visual Graphics Group, VGG-16 was more accurate than AlexNet at the time, and was soon adopted by researchers and industry for their image classification tasks. The VGG structure consists of different layers such as convolution layers, MaxPool layers, FCL and SoftMax layer. Fig. 1 is shown the overall VGG architecture. Figure shows that VGG CNN contains 2 main structures. Each structure consists of a number of connected convolutional layers and full-connected layers. The input image size is 224*224*3 (RGB image) and the size of the filter is 3*3. Extracts features from the image better. To reduce the number of parameters as well as to improve the network's ability to resist image distortion, use Maxpooling. ReLU was used as an activation function[25-29]. Fig. 1 illustrates the VGG-16 model structure.

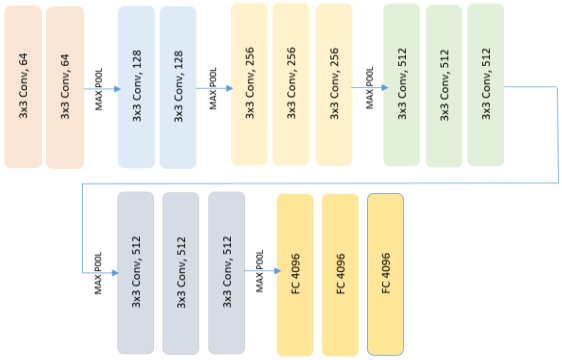

Fig. 1. VGG16 layers

All hidden layers use the ReLU equation, and the pattern is sequential and heavily dependent on a large number of filters at each level. On the downside, with 138 billion parameters, training times will be longer than with smaller models. In addition, there are models like the VGG19 that are modifications of the VGG16 (19 layers).

II. Realated work

Extracting the most relevant characteristics from medical pictures is the focus of medical image analysis, which aims to enhance clinical diagnosis. Making accurate positive and negative inferences from medical image classification models results in a trustworthy content-based image retrieval (CBIR) system[1], [2]. Numerous investigations have been performed to determine which categorization algorithms provide the most suitable and efficient retrieval system. [3], [4]. Using features derived from wavelet-based symmetric binary patterns, Ko *et al*. [5] analyzed a CBIR system using the random forest classifier. To further improve classification performance for medical condition detection, Qasem *et al*. [6] created a radial basis function network that generates its centers and weights concurrently using a multi-objective optimization technique. The technique was used to recover mammograms from a clinical setting. Breast thermograms may be analyzed using a technique devised [7] that relies on picture attributes. They suggested a neural network/support vector machine (SVM) hybrid multiple classifier approach and developed a fuzzy metric to evaluate the ensemble's diversity. In addition, CBIR has been integrated into a computer-aided diagnostic system. [8] to assist radiologists in the characterisation of mammographic masses. Image filtering, similarity fusion, and a relevance feedback technique were developed [9], as a means to retrieve medical pictures. In addition, they thought about supervised and unsupervised approaches to linking low-level and high-level characteristics for use in picture retrieval. However, [10] suggested a shape-texture feature extraction approach for categorizing radiological pictures. Due to the vast array of hyper parameters and algorithmic options, designing a deep convolutional neural network for a given issue is anything but simple. Another benefit of CNNs' lack of interpretability is that it allows them to be used with other well-studied signal processing methods. By breaking down an image into its component frequencies, the discrete wavelet transform (DWT) may aid in the feature extraction of a convolutional neural network (CNN). [11], [1]. There is a good theoretical consideration of the wavelet characteristics in multiresolution signal processing in CNNs. For instance, Williams *et al*. [12] supplied CNNs a fresh input consisting of the wavelet sub-bands of the original pictures. To top it all off, [13] suggested a wavelet scattering network as an alternative to ResNet's first hidden layer. The performance of this hybrid network is equivalent to that of ResNet, but with fewer hyper parameters. The challenge of organ tissue segmentation was also investigated by Lu *et al*. [14], who looked at a CNN enhanced with a dual-tree wavelet transform. To further subsample features, Williams *et al*. [15] developed a wavelet pooling approach based on a second-level wavelet decomposition. Recommended using convolutional neural networks (CNNs), discrete wavelet transforms (DWTs), and long short term memory (LSTM) together to identify liver and brain tumors. Additionally, we looked at a deep neural network by including multiresolution analysis derived from DWT.

While interesting in theory, this paper's invention of CAW and FAW hybrid transforms presents a difficult difficulty for broad applications. Simple CAW and FAW hybrid transformations need interpolation with the Arnold Transform for quick decomposition-based implementations to provide precise, completely rebuilt transforms. In addition, our approach yields a class of orthogonal bases for pictures. In terms of approximation and classifying pictures, numerical data demonstrate that the CAW and FAW hybrid transforms are superior than the wavelet transform.

III. The Proposed CAW and FAW Transforms

In this section the detail of cascading of several transform to produce hybrid transformation techniques is given. Such cascading will result in the present of the effect of these transform on the given input signals. As a first step in such combination after the application of the first transformation which is usually transfer the signal from the time domain to frequency domain, hence there will be a problem in the application of the next Transform. This is because the forward transformation always convert the signal from time domain to frequency domain and after application of first transformation the signal in the frequency domain hence it’s impossible to apply the second transform directly. Therefore it is necessary to search for a technique in order to overcome this problem, so it was used in these hybrid transformation the Arnold transform that scrambled frequency domain and keep the information. This facilitate the application of the next transform Fig. 2 illustrate flow chart of proposed system. In the following section the detail combination of tow schemes of mixing transforms, namely CAW and FAW will be given with demonstrated examples.

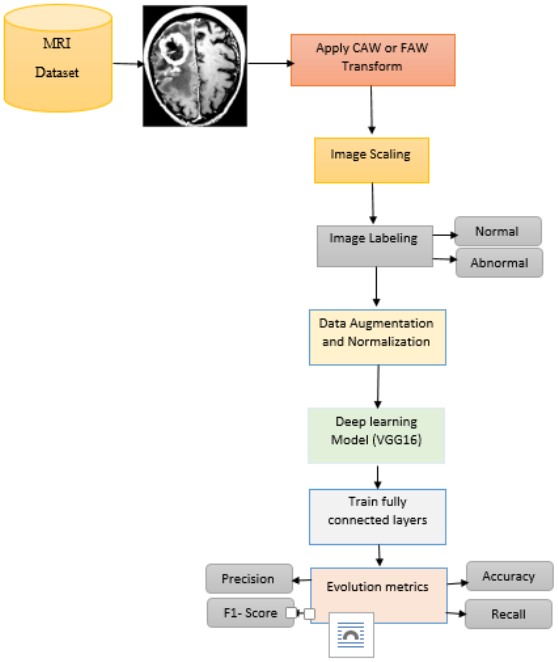

Fig. 2. Proposed System Flowchart

A. *CAW Transforms*

The main block diagram of the CAW mixed transform is given in Fig. 2. It consists of three steps namely:

Step1: Apply the discrete cosine transform (DCT).
Step2: Application of Arnold transform (AT).

The following procedure should be followed in the computation of AT:

- The application of DCT to the image X will result in Y.
- Produce randomly two matrices A&B of the same dimension as Y above. The elements of each matrix should be different values (no reputation). In order to simplify the procedure a numerical example will be considered here of only 2x2 elements for simplicity:

$$Y = \begin{bmatrix} 1 & 2 \\ 3 & 4 \end{bmatrix}, A = \begin{bmatrix} 7 & 6 \\ 3 & 5 \end{bmatrix}, and\ B = \begin{bmatrix} 3 & 1 \\ 4 & 8 \end{bmatrix}$$

- Scramble the elements of Y using the following expression:

$$G(i,j) = \begin{bmatrix} 1 & A(i,j) \\ B(i,j) & A(i,j).B(i,j)+1 \end{bmatrix} \cdot \begin{bmatrix} i \\ j \end{bmatrix} mod\ N + \begin{bmatrix} 1 \\ 1 \end{bmatrix}$$

$$G(1,1) = \begin{bmatrix} 1 & 7 \\ 3 & 22 \end{bmatrix} \cdot \begin{bmatrix} 1 \\ 1 \end{bmatrix} mod\ 2 + \begin{bmatrix} 1 \\ 1 \end{bmatrix} \rightarrow G = \begin{bmatrix} 2 & 1 \\ 3 & 4 \end{bmatrix}$$

$$G(1,2) = \begin{bmatrix} 1 & 6 \\ 1 & 7 \end{bmatrix} \cdot \begin{bmatrix} 1 \\ 2 \end{bmatrix} mod\ 2 + \begin{bmatrix} 1 \\ 1 \end{bmatrix} \rightarrow G = \begin{bmatrix} 2 & 1 \\ 3 & 4 \end{bmatrix}$$

$$G(2,1) = \begin{bmatrix} 1 & 2 \\ 4 & 41 \end{bmatrix} \cdot \begin{bmatrix} 2 \\ 1 \end{bmatrix} mod\ 2 + \begin{bmatrix} 1 \\ 1 \end{bmatrix} \rightarrow G = \begin{bmatrix} 2 & 3 \\ 1 & 4 \end{bmatrix}$$

$$G(2,2) = \begin{bmatrix} 1 & 5 \\ 8 & 4 \end{bmatrix} \cdot \begin{bmatrix} 2 \\ 2 \end{bmatrix} mod\ 2 + \begin{bmatrix} 1 \\ 1 \end{bmatrix} \rightarrow G = \begin{bmatrix} 4 & 3 \\ 1 & 2 \end{bmatrix}$$

- The position of elements of Y will be replaced as obtained to G. hence the application of next transformation will be applied on G instead of Y.
- Apply the discrete Wavelet transform (DWT).

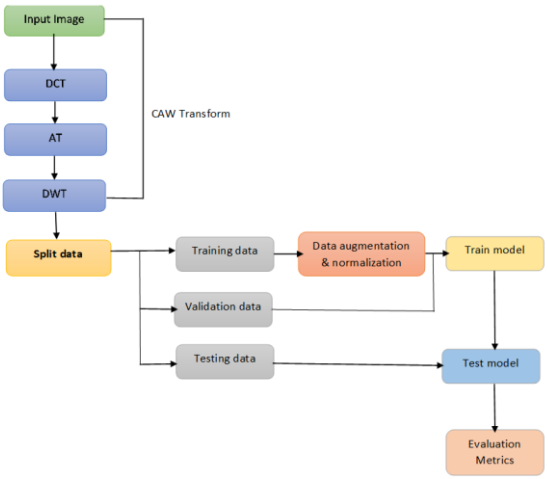

Fig. 3. CAW Transform diagram

B. *FAW Transforms*

The main block diagram of the CAW mixed transform is given in Fig. 3. It consists of three steps namely:

Step1: Apply the discrete Fourier transform (DFT).
Step2: Application of Arnold transform (AT).
Step3: Take a real part from the matrix result from AT let be called R
Step4: Take imaginary part from the matrix result from AT let be called I
Step5: find the Magnitude = √(R^2+I^2)
Step6: Apply the discrete Wavelet transform (DWT) on Magnitude.

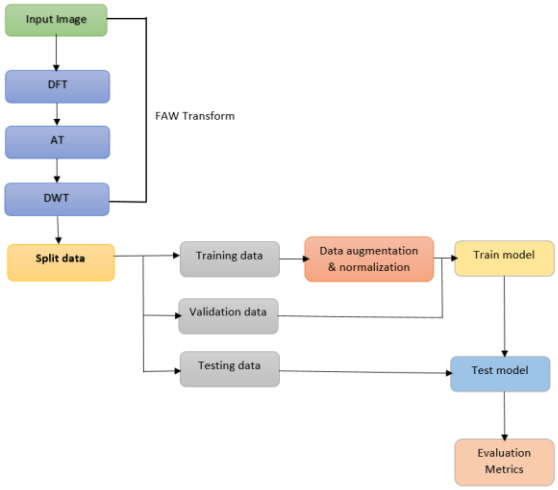

Fig. 4. FAW transform diagram

IV. Experiment Rustles

The effectiveness of Mixed CAW and FAW transformations in the medical picture domain was investigated by means of classification tasks. Both the accuracy with which the original picture can be reconstructed, and the efficiency of the feature extraction approach are taken into account for this comparison. Based on our first studies, using these mixed transforms projections to get a high classification rate is essential for achieving successful outcomes. However, owing to energy concentration, the resultant nonlinear approximation pictures are mostly constituted of the mixed transform functions that surround the edges, even if these transforms include most of the DCT or DFT type basis functions.

A. Databases

For this dataset, we compiled MRI scans of brain tumors from six different Kaggle databases; each of these databases included a collection of annotated images [30]. The first dataset included 253 MRI scans, split evenly between those without tumors (98) and those with malignancies (155). The second set of data, totaling 3,264 labeled photos, was broken down as follows: 926 images of glioma tumors, 937 images of meningioma tumors, 500 images of no tumor, and 901 images of pituitary tumors. The third database included 3,060 brain MRI pictures split into three groups: those with tumors (1,500), those without tumors (1,500), and those without labels (60). The total number of labeled photos in the fourth database was 7,023. These were likewise split into 4 distinct groups. There were 2,000 photographs in the third section without a tumor, 1,645 meningioma tumor images in the second section, 1,621 glioma tumor images in the first section, and 1,757 pituitary tumor images in the final section. The second set of data included 400 MRI pictures with labels, split evenly between normal (170) and tumor (115 230) cases. There were 2,501 pictures in the most recent brain MRI database, with 1,551 categorized as normal and 950 as stroke. We finally divide these data sets into two categories: typical and out-of-the-ordinary. We had 5,819 photos in the normal category and 10,622 in the abnormal category. That brings the total number of photos in this collection to 16,441 [30-33].

B. Evaluation Metrics Rustles

The proposed mixed transforms algorithms are tested using MATLAB for the performance evaluation. The evaluation of the proposed CAW and FAW transforms perform by using Tumor dataset, first we extract features by using proposed CAW and FAW transforms. We used the test and training data to determine the accuracy of the classification features retrieved in the 'Softmax' layers. Training data sets are described in detail using the technique. The two models were put to the test with a standard performance assessment (Sensitivity, Accuracy, Specificity, Precision, Recall,G mean and F Measure) The predicted results for the suggested CAW and FAW Transform model's behavior are shown in Table 1. There has been satisfactory accuracy in both the training and validation checks. After training the feature retrieved from transformations, the VGG16 model's accuracy and training loss are shown in Figs. 4 and 5, respectively.

Algorithm 1. Implement the major steps of proposed medical classification model.

Require: Data-base images Img={ $I_1,I_2,I_3,\ldots,I_n$} a label for Medical images must not similar on the other person and I ∈ Ì.

Training step:

- Extract features using CAW or FAW Transforms.
- Split feature Img into tow part (designset, testset).
- Split designset into tow part (Training (Trset), Validation (Valset)).
- Train (VGG16, Trset, Valset).
- Finish training when meeting the acceptance performance and criteria.
- Return: Train images.

Testing steps:

- Evaluation Train images by use metrics (prestion, recall, F1 measure, and G mean).
- Extract the features testset and testf for Ì at FC .
- Calculate the accuracy of system.
- End.

TABLE I. Evolution metrics of proposed CAW and FAW transforms on VGG16

Model	Accuracy	Sensitivity	Specificity	Precision	Recall	G-Mean	F1 Measure
CAW-VGG16	**0.9408**	**0.9512**	**0.9641**	**0.9450**	**0.9012**	**0.9819**	**0.9201**
FAW-VGG16	**0.9250**	**0.9104**	**0.9170**	**0.8821**	**0.9412**	**0.8771**	**0.8510**

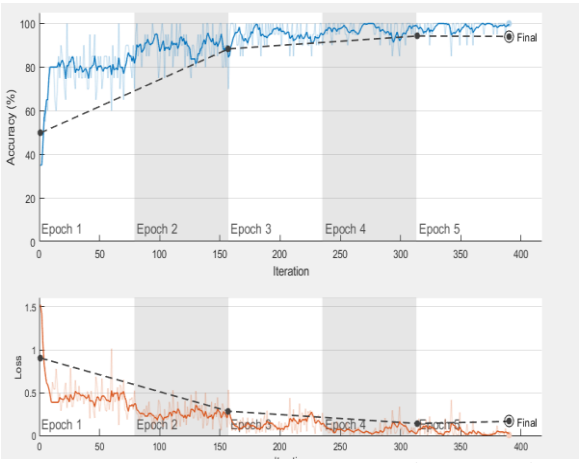

Fig. 5. Accuracy and loss rate of CAW classification.

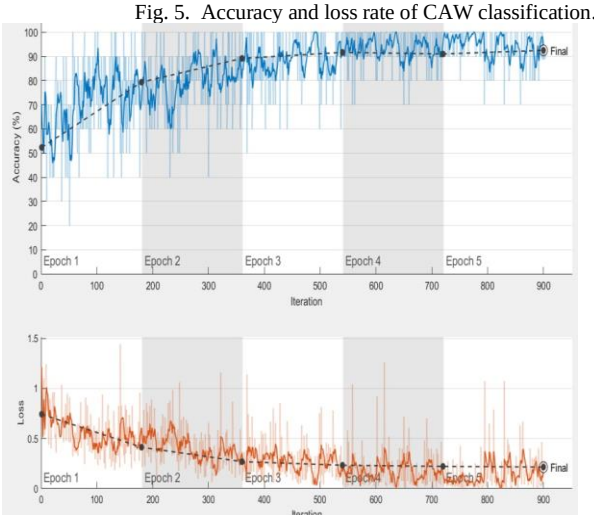

Fig. 6. Accuracy and loss rate of FAW classification

Tables 1 show that the proposed algorithm has an excellent robustness in feature extraction. These results showed the accuracy of the CAW transform after train on VGG16 model 94.08%, and for FAW transform 92.50%.

V. Conclusion

This study introduced the Arnold concept as the basis for a new family of picture transforms that combine discrete orthonormal transformations. The CAW and FAW mixed Transform algorithms are two new proposals. Initially, the DCT, AT, and DWT transforms were combined using the CAW mixed transform. The consolidated regulations derived by successively applying these transformations in sequence. The FFT, AT, and DWT were then combined to construct the FAW transform. The combined rules that result from applying these transformations in a chain. The effectiveness of these mixtures was evaluated using both subjective and objective criteria. The results proved our proposed strategy can better preserve source picture data and disclose more features after integration. Evidently, the suggested approach is reliable and productive in producing desirable fusion outcomes, which opens up several practical possibilities. Classification of medical images using several transforms is the topic of this research. However, the accuracy of medical picture categorization is inversely proportional to the processing speed in real time. Future research should focus on how to increase the method's efficiency while maintaining the same score rate of categorization outcomes.

As the DWT decomposition level rises, the method becomes less noticeable, which may boost its robustness. Energy may be compacted with the aid of DCT, and unnecessary features can be trimmed away from the extraction process in this way. Arnold transforms method is used to jumble picture pixels before inserting them as a spread spectrum pattern, which significantly strengthens the image's security and reliability. Using MATLAB, we verify the proposed algorithm's results and compare them to those of similar efforts. Simulation results demonstrate the superior performance and great accuracy of the suggested method.

Acknowledgments

The research behind this paper would not have been possible without the exceptional support of Prof. Waleed AlJawher. Throughout researching image processing journals and writing this paper, He have inspired me with them enthusiasm, knowledge, and attention to detail.

References

[1] Khatami, A., Babaie, M., Tizhoosh, H. R., Khosravi, A., Nguyen, T., & Nahavandi, S. (2018). A sequential search-space shrinking using CNN transfer learning and a Radon projection pool for medical image retrieval. *Expert systems with applications*, *100*, 224-233.

[2] Waheed, S. R., Rahim, M. S. M., Suaib, N. M., & Salim, A. A. (2023). CNN deep learning-based image to vector depiction. *Multimedia Tools and Applications*, 1-20.

[3] Alsmadi, M. K. (2020). Content-based image retrieval using color, shape and texture descriptors and features. *Arabian Journal for Science and Engineering*, *45*(4), 3317-3330.

[4] Waheed, S. R., Suaib, N. M., Rahim, M. S. M., Adnan, M. M., & Salim, A. A. (2021, April). *Deep Learning Algorithms-based Object Detection and Localization Revisited. Journal of Physics: Conference Series (Vol. 1892*, No. 1, p. 012001). IOP Publishing.

[5] Ko, B. C., Kim, S. H., & Nam, J. Y. (2011). X-ray image classification using random forests with local wavelet-based CS-local binary patterns. *Journal of Digital Imaging*, *24*, 1141-1151.

[6] Hathot, S. F., Jubier, N. J., Hassani, R. H., & Salim, A. A. (2021). Physical and elastic properties of TeO_2-Gd_2O_3 glasses: Role of zinc oxide contents variation. *Optik*, *247*, 167941.

[7] Krawczyk, B., & Schaefer, G. (2014). A hybrid classifier committee for analysing asymmetry features in breast thermograms. *Applied Soft Computing*, *20*, 112-118.

[8] Tsochatzidis, L., Zagoris, K., Arikidis, N., Karahaliou, A., Costaridou, L., & Pratikakis, I. (2017). Computer-aided diagnosis of mammographic masses based on a supervised content-based image retrieval approach. *Pattern Recognition*, *71*, 106-117.

[9] Salim, A. A., Bidin, N., & Islam, S. (2017). Low power CO2 laser modified iron/nickel alloyed pure aluminum surface: Evaluation of structural and mechanical properties. *Surface and Coatings Technology*, *315*, 24-31.

[10] Mohammadi, S. M., Helfroush, M. S., & Kazemi, K. (2012). Novel shape-texture feature extraction for medical X-ray image classification. *Int J Innov Comput Inf Control*, *8*, 659-76.

[11] Adnan, M. M., Rahim, M. S. M., Al-Jawaheri, K., Ali, M. H., Waheed, S. R., & Radie, A. H. (2020, September). A survey and analysis on image annotation. *2020 3rd International Conference on Engineering Technology and its Applications (IICETA)* (pp. 203-208). IEEE.

[12] Abbas, A. M., Abid, M. A., Abbas, K. N., Aziz, W. J., & Salim, A. A. (2021, April). Photocatalytic activity of Ag-ZnO nanocomposites integrated essential ginger oil fabricated by green synthesis method. *Journal of Physics: Conference Series (Vol. 1892*, No. 1, p. 012005). IOP Publishing.

[13] Oyallon, E., Belilovsky, E., & Zagoruyko, S. (2017). Scaling the scattering transform: Deep hybrid networks. *Proceedings of the IEEE international conference on computer vision* (pp. 5618-5627).

[14] Lu, H., Wang, H., Zhang, Q., Won, D., & Yoon, S. W. (2018, June). A dual-tree complex wavelet transform based convolutional neural network for human thyroid medical image segmentation. *2018 IEEE international conference on healthcare informatics (ICHI)* (pp. 191-198). IEEE.

[15] Williams, T., & Li, R. (2018, May). Wavelet pooling for convolutional neural networks. *International Conference on Learning Representations*.

[16] Salim, A. A., Bakhtiar, H., Bidin, N., & Ghoshal, S. K. (2018). Unique attributes of spherical cinnamon nanoparticles produced via PLAL technique: Synergy between methanol media and ablating laser wavelength. *Optical Materials*, *85*, 100-105.

[17] Amana, M. S., Aldhuhaibat, M. J. R., & Salim, A. A. (2021). Evaluation of the absorption, scattering and overall probability of gamma rays in lead and concrete interactions. *SCIOL Biomed*, *4*, 191-199.

[18] Mahmoud, W. A. (2021). Computation of Wavelet and Multiwavelet Transforms Using Fast Fourier Transform. *Journal Port Science Research*, *4*(2), 111-117.

[19] Masadeh, R., Mahafzah, B. A., & Sharieh, A. (2019). Sea lion optimization algorithm. *International Journal of Advanced Computer Science and Applications*, *10*(5).

[20] Ahmed, N., Natarajan, T., & Rao, K. R. (1974). Discrete cosine transform. *IEEE transactions on Computers*, *100*(1), 90-93.

[21] Potts, D., Steidl, G., & Tasche, M. (2000). Fast Fourier transforms for nonequispaced data: A tutorial, chapter 12.

[22] Min, L., Ting, L., & Yu-jie, H. (2013, November). Arnold transform based image scrambling method. *3rd International Conference on Multimedia Technology (ICMT-13)* (pp. 1302-1309). Atlantis Press.

[23] Nussbaumer, H. J., & Nussbaumer, H. J. (1981). *The fast Fourier transform* (pp. 80-111). Springer Berlin Heidelberg.

[24] Salim, A. A., Bakhtiar, H., Bidin, N., & Ghoshal, S. K. (2018). Antibacterial activity of decahedral cinnamon nanoparticles prepared in honey using PLAL technique. *Materials Letters*, *232*, 183-186.

[25] Xiao, J., Wang, J., Cao, S., & Li, B. (2020, April). Application of a novel and improved VGG-19 network in the detection of workers wearing masks. *Journal of Physics: Conference Series* (Vol. 1518, No. 1, p. 012041). IOP Publishing.

[26] Alzubaidi, L., Zhang, J., Humaidi, A. J., Al-Dujaili, A., Duan, Y., Al-Shamma, O., ... & Farhan, L. (2021). Review of deep learning: Concepts, CNN architectures, challenges, applications, future directions. *Journal of Big Data*, *8*, 1-74.

[27] Ramli, N. S., Sazali, E. S., Mahraz, Z. A., Ghoshal, S. K., Zain, S. M., Hisam, R., ... & Salim, A. A. (2023). Hard tissue repairing potency of mesoporous borosilicate bioactive glass: An in vitro assessment. *Journal of Non-Crystalline Solids*, *609*, 122289.

[28] A. A Salim, Ghoshal, S. K., & Bakhtiar, H. (2022). Prominent absorption and luminescence characteristics of novel silver-cinnamon core-shell nanoparticles prepared in ethanol using PLAL method. *Radiation Physics and Chemistry*, *190*, 109794.

[29] Rai, H. M., & Chatterjee, K. (2021). 2D MRI image analysis and brain tumor detection using deep learning CNN model LeU-Net. *Multimedia Tools and Applications*, *80*, 36111-36141.

[30] Vernooij, M. W., Ikram, M. A., Tanghe, H. L., Vincent, A. J., Hofman, A., Krestin, G. P., ... & van der Lugt, A. (2007). Incidental findings on brain MRI in the general population. *New England Journal of Medicine*, *357*(18), 1821-1828.

[31] Kadhim, K. A., Najjar, F. H., Waad, A. A., Al-Kharsan, I. H., Khudhair, Z. N., & Salim, A. A. (2023). Leukemia Classification using a Convolutional Neural Network of AML Images. *Malaysian Journal of Fundamental and Applied Sciences*, *19*(3), 306-312.

[32] Waheed, S. R., Saadi, S. M., Rahim, M. S. M., Suaib, N. M., Najjar, F. H., Adnan, M. M., & Salim, A. A. (2023). Melanoma Skin Cancer Classification based on CNN Deep Learning Algorithms. *Malaysian Journal of Fundamental and Applied Sciences*, *19(*3), 299-305.

[33] Waheed, S. R., Sakran, A. A., Rahim, M. S. M., Suaib, N. M., Najjar, F. H., Kadhim, K. A., Salim, A. A. & Adnan, M. M. (2023). Design a Crime Detection System based Fog Computing and IoT. *Malaysian Journal of Fundamental and Applied Sciences*, *19*(3), 345-354.